Localisation of Acoustic Emission in Reinforced Concrete Using Heterogeneous Velocity Models

Stephan GOLLOB *[1], Thomas VOGEL *
* ETH Zürich, Zürich, Switzerland
[1]gollob@ibk.baug.ethz.ch

Abstract. Acoustic emission analysis (AEA) has become a promising method to monitor the change in the condition of concrete structures. The research project aims at investigating the influence of reinforcement and cracks on wave propagation.

Therefore, localisation algorithms using heterogeneous velocity models are developed. Taking the heterogeneity of concrete and the influence of reinforcement into account will improve the source localisation accuracy. Until now it is common to use homogeneous velocity models to localize the acoustic emission (AE) source. As a consequence effects of heterogeneity, especially reinforcements, and cracks cannot be considered. Therefore, a new numerical reinforced concrete model (NRCM) is developed which is used to investigate the influence of reinforcements and cracks on the wave propagation path and their influence on the signal recorded by piezoelectric sensors.

As a rule the reinforcement layout is known. Otherwise, the layout can be determined using acoustic tomography for example. The only information provided by the velocity model of the specimen is the wave velocity of each voxel depending on the assigned material. A localization method is modified for processing these heterogeneous velocity models. The source location is calculated iteratively. The difference between the calculated signal arrival time and the measured arrival time is used to update the estimated source location and time. It is common to use one homogeneous wave velocity, the distance between the estimated source location and a sensor as well as the estimated source time, to compute the calculated arrival time. Using the heterogeneous velocity model, the wave travel time between the estimated source location and a sensor can be calculated as sum of the wave travel times through every voxel assuming a linear wave propagation path.

An acoustic tomogram could be updated using the data recorded by the sensors monitoring the specimen. Hence, also the velocity model could be updated. Cracks could be considered in the velocity model, even if they occur after the preliminary tomography. The combination of three dimensional acoustic tomography with AE analysis is a novel and promising approach.

Introduction

The heterogeneity of concrete and in particular the reinforcement bars in reinforced concrete have an influence on wave propagation. However, it is common to use homogeneous velocity models to localize AE sources. The objective of the work discussed in this document is to establish a heterogeneous velocity model for source localization.

License: http://creativecommons.org/licenses/by-nd/3.0/

1. Numerical Simulations

A number of numerical elastic wave propagation simulations have been performed to investigate the influence of heterogeneity and reinforcement on wave propagation. Furthermore, the recorded data was used to create and calibrate a three-dimensional source localisation algorithm, based on a heterogeneous velocity model.

1.1 Numerical Model

The modelled specimen is discretized into voxels with the shape of a cube and the side length of 1 gp (grid point). The size of the cubical voxels specifies the level of discretization of the numerical specimen. In the simulations, 1 gp was defined to equal 1 mm. Thus, everything with the size of one millimeter or more can be considered within the numerical model. Anything smaller than one millimeter cannot be considered. Similar numerical simulations have demonstrated that such a limitation does not significantly influence the results [3].

The simulated specimen (Pic. 1) consist out of a concrete rectangular cuboid surrounded by air. Reinforcement bars can be modelled too. In case of some of the simulations, a bar with a diameter of $d = 30$ gp is located at the center of the concrete cuboids and oriented in the z-direction.

Reinforcement steel is a homogeneous material, whereas the concrete is heterogeneous. The most important components of concrete are cement, aggregates and air voids. The air voids and the aggregate grains are randomly, but evenly, distributed. Thus, it is possible to calculate homogeneous effective elastic properties (EEP) [2] for the heterogeneous material concrete. The numerical construction materials used for the simulations are air, reinforcement steel and EEP concrete. The material properties required for this model are the p-wave velocity, the s-wave velocity and the density of the materials.

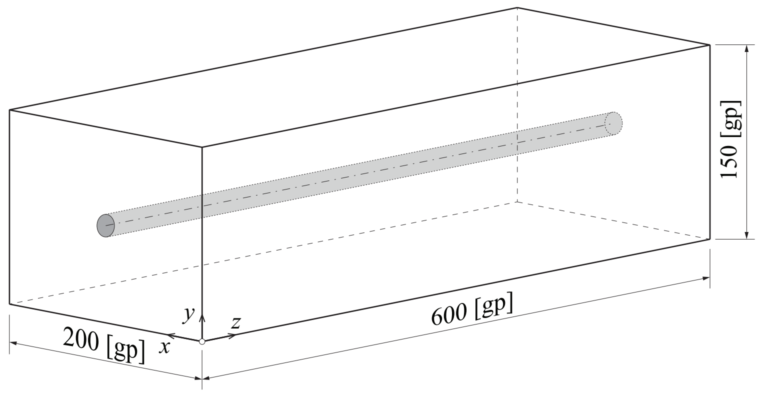

Pic. 1. Numerical generated specimen including one reinforcement bar of diameter $d = 30$ gp

1.2 Wave Propagation

The elastic wave propagation is calculated using a FORTRAN® application (Heidimod 6.4), developed by E. H. Saenger, based on a modified finite-difference grid [4]. The calculated wave propagation can be visualized. The displacements of the voxels in z-direction for a cross section at $y = 75$ mm after 24 µs are displayed in Pic. 2. The source is located in the steel bar at $x = 100$, $y = 75$ mm and $z = 150$ mm and marked with ✳.

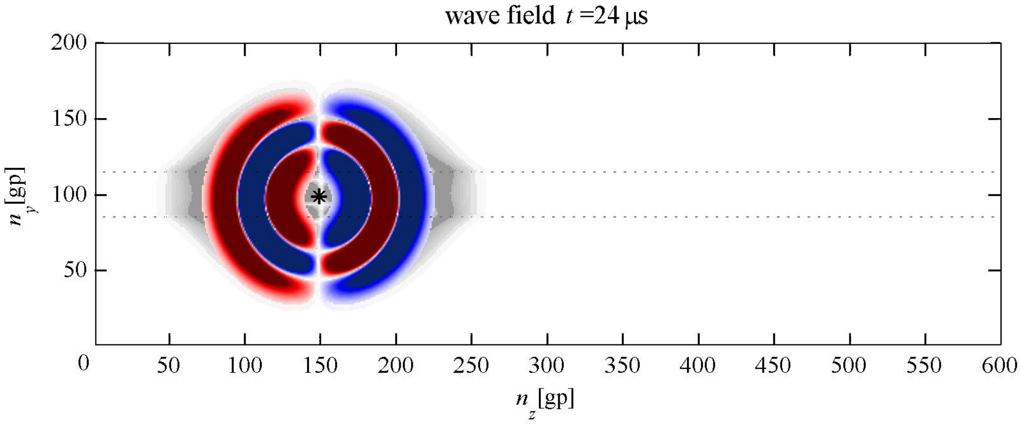

Pic. 2. Displacement field in the z-direction after 24 μs at cross section $y = 75$ mm.
The source location is marked with ✳.

The displacements of the voxels calculated for an unreinforced concrete model is visualized with colors of different intensity. The displacement in the positive z-direction is visualized in shades of blue, whereas the displacement in the negative z-direction is visualized in shades of red. The displacement calculated for a reinforced concrete model is visualized in shades of gray. The edges of the reinforcement bar are marked with dashed lines. The influence of the reinforcement on the wave propagation is clearly illustrated by the plot.

2. Source Localization

44 numerical sensors are modelled to measure the displacements caused by an artificial source. The recorded signals have subsequently been used to determine the source location.

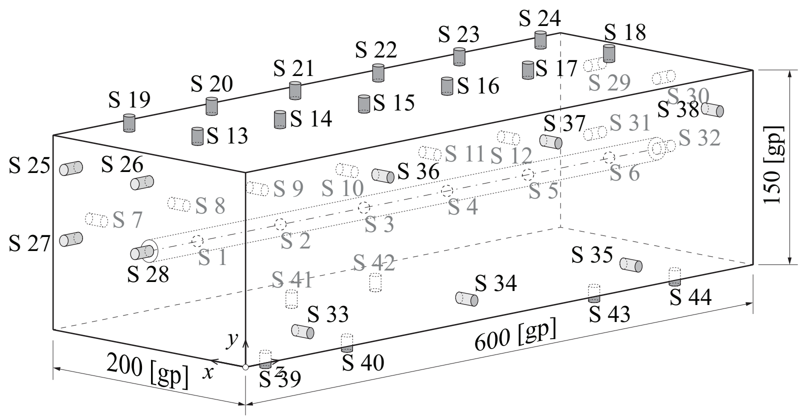

Pic. 3. Sensor arrangement

The arrival times of the wave at the sensors are determined from the recorded displacement history. A fixed threshold was used to pick the arrival times. For determining the source location it is common to use a homogeneous velocity model. This is only true if the specimen is composed out of one homogeneous material. However, the equations presented in section 2.1 are also used to determine the source location in heterogeneous materials.

2.1 Three-Dimensional Source Localization for Homogeneous Materials

For every sensor the equation (1) should be fulfilled. The coordinates of each sensor i are x_i^S, y_i^S and z_i^S and the picked arrival time of the wave at this sensor t_i^A are known values.

$$t_i^A = \frac{\sqrt{\left(x_i^S - x_c\right)^2 + \left(y_i^S - y_c\right)^2 + \left(z_i^S - z_c\right)^2}}{c_p} + t_c \tag{1}$$

The homogeneous distributed wave velocity c_p is also known. The unknowns are the location of the source (x_c, y_c and z_c) as well as the source time t_c. A theoretical arrival time of the wave at each sensor could be calculated using some initial values for the source location and time. In general, the calculated time t_i^A is different to the measured one $t_i^{A,m}$.

$$\Delta t_i^A = t_i^{A,m} - t_i^A \tag{2}$$

The measured arrival time can also be written as

$$t_i^{A,m} = t_i^A + \Delta t_i^A = t_i^A + \frac{\partial f_i}{\partial x}\Delta x + \frac{\partial f_i}{\partial y}\Delta y + \frac{\partial f_i}{\partial z}\Delta z + \frac{\partial f_i}{\partial t}\Delta t \tag{3}$$.

where f_i is the right site of equation (1). The matrix form for N sensors of (3) can be formulated as

$$\begin{bmatrix} \Delta t_i^A \\ \vdots \\ \Delta t_N^A \end{bmatrix} = \begin{bmatrix} \frac{\partial f_1}{\partial x} & \frac{\partial f_1}{\partial y} & \frac{\partial f_1}{\partial z} & \frac{\partial f_1}{\partial t} \\ \vdots & \vdots & \vdots & \vdots \\ \frac{\partial f_N}{\partial x} & \frac{\partial f_N}{\partial y} & \frac{\partial f_N}{\partial z} & \frac{\partial f_N}{\partial t} \end{bmatrix} \cdot \begin{bmatrix} \Delta x \\ \Delta y \\ \Delta z \\ \Delta t \end{bmatrix} \tag{4}$$

or in compact matrix notation,

$$\Delta \boldsymbol{t^A} = \boldsymbol{F} \cdot \Delta \boldsymbol{s} \tag{5}$$

where $\boldsymbol{\Delta t^A}$ and $\boldsymbol{F}$ are known. The vector of the correction values $\Delta\boldsymbol{s}$ is unknown. With four sensors ($N = 4$) the solution of (5) is well defined.

$$\Delta \boldsymbol{s} = \boldsymbol{F}^{-1} \cdot \Delta \boldsymbol{t^A} \tag{6}$$

It is impossible to solve the equation with less than four sensors. If $N > 4$, the equation is over-determined. In this case a least square approximation is used.

$$\Delta \boldsymbol{s} = (\boldsymbol{F}^T \cdot \boldsymbol{F})^{-1} \cdot \boldsymbol{F}^T \cdot \Delta \boldsymbol{t^A} \tag{7}$$

It is preconditioned that the model parameters are independent and the data inaccuracies are normally distributed. Due to the linearization of the problem, the solution can be calculated iteratively. The solution of (7) is used to update the source coordinates for the next iteration step, k+1.

$$\begin{aligned} {x_c}^{(k+1)} &= {x_c}^{(k)} + R_x \cdot \Delta x \\ {y_c}^{(k+1)} &= {y_c}^{(k)} + R_y \cdot \Delta y \\ {z_c}^{(k+1)} &= {z_c}^{(k)} + R_z \cdot \Delta z \\ {t_c}^{(k+1)} &= {t_c}^{(k)} + R_t \cdot \Delta t \end{aligned} \tag{8}$$

The R_j' values are relaxation parameters, which should be between zero and one. These values can be different for each source parameter. All four relaxation parameters are set to 0.01 for all iterative localisation calculations mentioned in this document. The iteration process is finished when all update parameters $R_j \cdot \Delta j$ are smaller than a certain threshold $\boldsymbol{\varepsilon}$. In case of the simulations ε is equal to 0.25. The described source localization algorithm is described in [1] and [5].

2.2 Three-Dimensional Source Localization for Heterogeneous Materials

The p-wave velocity c_p is a material property. In heterogeneous specimens, c_p is not a constant value. An average wave velocity $c_{p,i}$ for the wave travel path between source and each sensor is needed to fulfill equation (1). This average wave velocity has to be determined for each sensor and each step of the iteration process. Considering the average p-wave velocity, equation (1) changes to

$$t_i^A = \frac{\sqrt{\left(x_i^S - x_c\right)^2 + \left(y_i^S - y_c\right)^2 + \left(z_i^S - z_c\right)^2}}{c_{p,i}} + t_c \quad (9).$$

A discretized velocity model of the specimen is used to determine the average p-wave velocities. In these simulations the discretization of the numerical model of the specimen used for calculating the average p-wave velocity between the source and a sensor is identical to the discretization of the numerical model applied to the wave propagation simulation mentioned before. For the discretization, a lower bound to the voxel size should be taken as 1 mm^3. The dimensions used provide a good resolution for the specimen containing the reinforcement bar. A higher resolution will not lead to a more accurate result. It will however, significantly increase the computational time. The p-wave velocity for each voxel is the only information contained in the numerical velocity model.

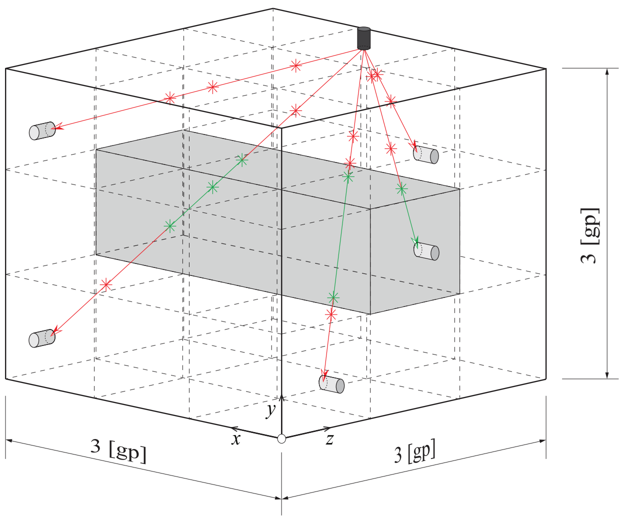

Pic. 4. Cube with an edge length of 3 gp, one transmitter (black) and five sensors (gray). Two different materials are illustrated in gray and white. The direct wave travel path between transmitter and the five sensors (receivers) through the specimen is illustrated. The intersections of the wave travel path and the voxel surfaces are marked with a ✳.

In order to calculate the average wave velocity, the voxels containing the direct beam between source and sensor have to be identified and der number j_i determined. The length $l_{v,ji}$ of the partial segments of the beam inside each voxel j must also be determined. The average p-wave velocity $c_{p,i}$ on the path between sensor i and the estimated source location can subsequently be calculated.

$$c_{p,i} = \frac{\sum_{j=1}^{j_i}\left(c_{p,j} \cdot l_{V,ji}\right)}{l_i} \quad (10)$$

The calculated average p-wave velocity will be used as input for equation (9). Despite calculating an average velocity, the iterative determination of the source location is identical to the process described for homogenous specimens in the section 2.1 starting with equation (2).

This method implies a straight wave propagation path. For an inhomogeneous specimens this is a simplification. Consequently, every possible wave propagation path starting from each sensor should be determined for example by using time reverse modelling [2]. However, the computational effort for time reverse modeling is high and the result of the calculation does not always provide a clear source location. By assuming a straight wave propagation path, which is an appropriate simplification, the computational effort can be significantly reduced.

2.3 Fast Three-Dimensional Source Localization for Heterogeneous Materials

In order to speed up the localization, it is performed in two phases. A preliminary localization is carried out using the three-dimensional source localization for homogeneous materials. In reinforced concrete, the majority of the specimen volume consist of concrete. Therefore, only the p-wave velocity of the EEP concrete is used. Any point within the specimen can be chosen as initial assumption for the source location.

A localization using the discretized (heterogeneous) velocity model is performed in the second phase. The source location determined during phase one is used as an initial assumption for this phase. Moreover, the threshold ε is reduced to half of the value defined for phase one. This phase lasts about additional 50 times longer than the first one.

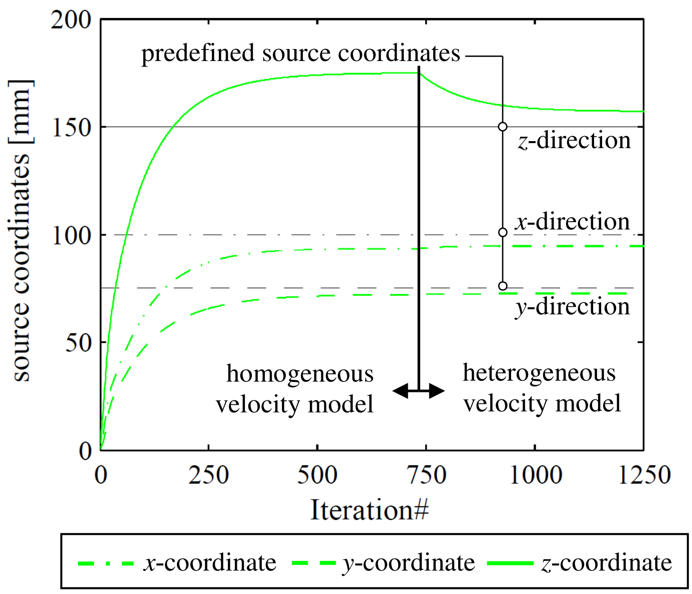

Pic. 5. The development of the iterative source location in two phases; using a homogeneous and a heterogeneous velocity model.

Pic. 5 illustrates the iterative progress of the determination of the source location. The predefined source location for the forward simulation is $x = 100$ mm, $y = 75$ mm and $y = 150$ mm. These coordinates are marked with blacks lines. The initial assumption for the source location was $x = 0$ mm, $y = 0$ mm and $z = 0$ mm. The discontinuity of the graphs after the first 743 iteration steps indicates the change of the velocity model. By changing the velocity model, the accuracy of the calculated source location improves significantly. Especially the error the in z-direction, corresponding to the direction of the reinforcement bar axis, could be reduced clearly (71% error reduction). However, the source time calculated using the complex velocity model indicates a greater difference to the predefined source time than the final iteration step using the homogeneous model. In general, the accurate determination of the source location is more important than determining the exact source time. Moreover, the source time error is still within the range of microseconds.

2.4 Advantages and Limitations of the Heterogeneous Velocity Model

The discretized heterogeneous velocity model enables the simulation of any reinforcement layout. This method is not limited to reinforced concrete and can be used for any material and material composition. Moreover, the method can be used for different structures.

A material of particular interest is (numerical) air as it does not transmit the wave. The wave is reflected entirely if it encounters air. This modelling assumption corresponds to the real physical behavior. Small air voids within the specimen, as they naturally occur in concrete, are no problem for the discretized heterogeneous velocity model. The calculated average p-wave velocity $c_{p,i}$ will be reduced due to the fact that the assigned p-wave velocity of the voxels representing air is zero (equation (10)). A physical as well as a numerical wave has to bypass the air void and the time needed to travel from the source to the sensor increases. In concrete, the air void dimensions are in the range of one millimeter. Hence, this detour of the wave traveling path is relatively small. Strictly speaking, those detours do not change the p-wave velocity, they change the wave propagation path. In case of cracks this detour can become significantly longer. Equation (10) assumes a linear wave travel path. In uncracked specimens this is an appropriate simplification. In case of cracked specimens this assumption, however, leads to inaccurate results. Even with cracked specimens, the heterogeneous wave velocity model still provides a more accurate solution than the homogeneous model.

3. Conclusions and Outlook

A discretized heterogeneous velocity model provides an appropriate way to consider the different wave velocities in heterogeneous specimens. The accuracy of the source localization can be increased significantly. The result of the iterative source localization can, however, only be an approximation of the real source location. The quality of the result depends strongly on the sensor arrangement, the quality of the recorded data and the accuracy of the picked arrival time of the wave at each sensor.

A discretized velocity model can reflect every composition of a specimen. However, the calculation of the average p-wave velocity is time consuming. By calculating an estimated source location using a homogeneous velocity model and using the result as initial source location for the heterogeneous source localization, the computational time can be reduced significantly. The initial guessed source location used for the homogeneous iteration should only have a minor impact on the finally calculated source location. The computational time needed to calculate the average velocity $c_{p,i}$ between the estimated source location and a sensor depends on the number of voxels j_i passed through by a beam connecting the source and sensor directly. Hence, the choice of the discretization level is critical. The voxels should not be smaller than 1 mm^3. The diameters of the reinforcement bars typically vary between 6 mm and a few centimeters. Hence, 1 cm^3 voxels should be considered as an absolute upper boundary to model reinforced concrete. If cracks, air voids and/or small aggregate grains are to be considered, the size of the voxels should not be larger than a few cubic millimeters.

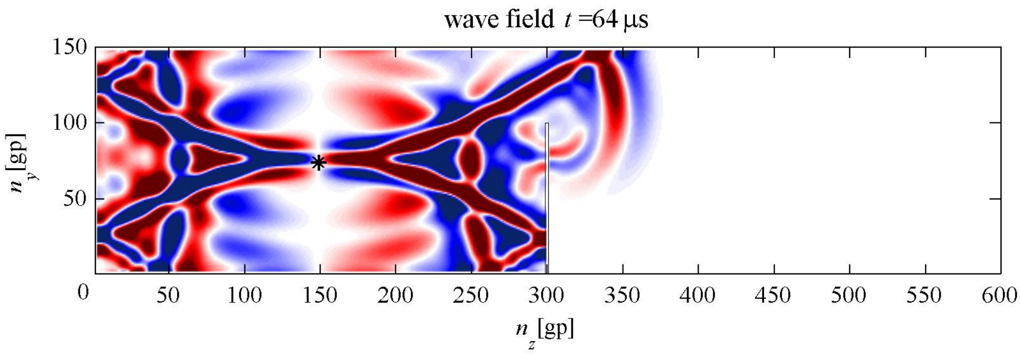

Pic. 6. Displacement field in the z-direction within an unreinforced concrete specimen after 64 µs at cross section x = 100 mm. The source location is marked with a ✳.

Reinforced concrete is usually a cracked material. These cracks are commonly located within the regions where AE's occur. The elastic wave induced by the AE source is nearly entirely reflected at the crack surface and not transmitted (Pic. 6). The wave travel path to the opposite side of the crack leads around the crack and does not remain straight. Equations (1) and (9) consider only straight wave propagation paths.

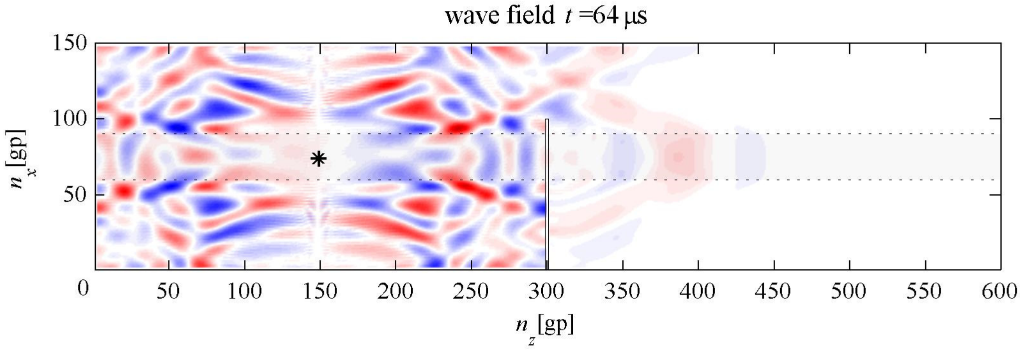

Pic. 7. Displacement field in the z-direction within a reinforced concrete specimen after 64 µs at cross section $x = 100$ mm. The source location is marked with a ✳.

Reinforcement bars passing through the cracks guide the elastic wave and therefore minimize the effect of the crack on wave propagation (Pic. 7).

The simulations performed indicate that discretized velocity models significantly improve the localization accuracy in heterogeneous specimens. The development of a velocity model, which is capable of considering cracks, is the next logical step.

Acoustic tomography could be used to determine a discretized velocity model of a specimen. Moreover, the data gained during the acoustic emission measurement could be used to update the tomogram. Cracks could be considered in the velocity model even if they occur during the AE monitoring.

References

[1] Christian U. Grosse and Masayasu Ohtsu, editors. *Acoustic Emission Testing, Basics for Research - Applications in Civil Engineering*. Springer-Verlag Berlin Heidelberg, 2008.

[2] Georg Karl Kocur. *Time reverse modeling of acoustic emission in structural concrete*. PhD thesis, ETH Zürich, 2012.

[3] Georg Karl Kocur, Erik H. Saenger, and Thomas Vogel. Elastic wave propagation in a segmented X-ray computed tomography model of a concrete specimen. *Construction and Building Materials*, 24:2393–2400, 2010.

[4] Erik H. Saenger, Norbert Gold, and Serge A. Shapiro. Modeling the propagation of elastic waves using a modified finite-difference grid. *Wave Motion*, 31(1):77–92, 2000.

[5] Frank Schubert. Basic principles of acoustic emission tomography. *J. Acoustic Emission*, 22:147–157, 2004.